JOURNAL OF GEOPHYSICAL RESEARCH, VOL. 93, NO. C3, PAGES 2227–2236, MARCH 15, 1988

Gulf Stream Velocity Structure Through Inversion of Hydrographic and Acoustic Doppler Data

STEPHEN D. PIERCE[1] AND TERRENCE M. JOYCE

Woods Hole Oceanographic Institution, Woods Hole, Massachusetts

Near-surface velocities from a shipborne acoustic Doppler instrument are used together with conductivity-temperature-depth and O_2 data to make estimates of geostrophic velocities off of Cape Hatteras. The data set consists of two transects across the Gulf Stream at approximately 73°W and 71°W made by the R/V *Endeavor* in August 1982. An inversion technique is applied which makes use of both the acoustic Doppler data and property conservation requirements. The method produces estimates of the absolute flow field across the two sections with formal errors of 1–2 cm/s. At the time of the observations, the net Gulf Stream transports are estimated to be $116 \pm 2 \times 10^9$ kg/s at 73°W and $161 \pm 4 \times 10^9$ kg/s at 71°W. A southwestward Deep Western Boundary Current transport is estimated at $4 \pm 1 \times 10^9$ kg/s. Taken together with recent Gulf Stream transport estimates of similar accuracy made in June 1982, the results are in general larger than historical transport estimates in this region.

1. Introduction

A better understanding of the Gulf Stream is of obvious importance to an improved picture of the North Atlantic circulation. Although the Gulf Stream has been the most intensively studied of all western boundary currents, our knowledge of its velocity structure and transport remains rudimentary. This is especially true downstream of Cape Hatteras, where the Gulf Stream turns offshore and becomes more variable in time and space. The Gulf Stream increases in transport from 30 Sv at the Florida Straits to a maximum of about 150 Sv south of Nova Scotia [*Knauss*, 1969; *Worthington*, 1976]. This increase is part of a recirculation regime in the NW Atlantic which is not well defined by existing observations.

Any level of no motion method in this region of intensity and variability tends to be an especially poor assumption. Attempts have been made at better velocity estimates through the use of transport floats [e.g., *Richardson and Knauss*, 1971], transport profilers [e.g., *Halkin and Rossby*, 1985], or discrete current meters [e.g., *Hall*, 1985]. An inherent drawback with any of these methods is the relatively wide spacing of the current measurements, which can lead to spatial aliasing. The time and expense associated with these techniques necessitates a compromise in spatial resolution.

The ship-mounted acoustic Doppler instrument used in the present study has the advantage of providing dense spatial coverage of near-surface velocities. These absolute velocities may then be used to reference geostrophic calculations throughout the water column; the spatial resolution is limited only by the hydrographic station spacing. During the study of warm-core ring 82B, from August 20 to 25, 1982, two conductivity-temperature-depth (CTD)/O_2 sections across the Gulf Stream were made on R/V *Endeavor* cruise EN88 (Figure 1). To reduce the errors associated with the Doppler data, the geometry of the two transects allows transport budgeting constraints to be imposed, suggesting the use of inverse techniques [*Wunsch*, 1978].

This combination of acoustic Doppler data with inverse methods was recently used by *Joyce et al.* [1986] (hereinafter referred to as JWP) applied to the EN86 Gulf Stream sections made in June 1982. The success of the method with the EN86 data encouraged us to apply it to the similar EN88 data set. In both cases the combined inversion technique makes use of all of the available information, both the CTD/O_2 and the acoustic Doppler data, to produce the best estimate of the synoptic circulation in the region.

2. Data Description

As part of the study of warm-core ring 82B off of Cape Hatteras, a series of four transects were made to identify the water mass characteristics of the "undisturbed" regions on either side of the ring [*Olson et al.*, 1985]. The two sections made in June 1982 have been described by JWP. The present study analyzes the two hydrographic sections made by R/V *Endeavor* cruise EN88 from August 20 to 25, 1982, at approximately 73°W and 71°W (Figure 1). The CTD/O_2 data were collected and processed by the Woods Hole Oceanograhic Institution (WHOI) CTD group using an NBIS underwater unit. Acoustic Doppler data were collected with a ship-mounted 300-kHz Ametek-Straza instrument. A full description of the acoustic Doppler system is given by *Joyce et al.* [1982].

The raw Doppler data were averaged into 10-min bins and combined with LORAN navigation to yield absolute velocities relative to the Earth. Vertical averaging bins of 6.4-m thickness were used, and data from four bins between 60 m and 100 m were ultimately used in the reference velocity calculation. Data from depths shallower than this might be affected by an ageostrophic surface mixed layer, while below 100 m the quality of the Doppler data drops off sharply. Figure 1 shows some representative velocity vectors from the 60-m depth bin, edited for clarity. Data from the various depths are translated to a common level of 100 dbar via the thermal wind. Between each CTD station pair, components of the vectors perpendicular to the station pair are combined to yield a single normal reference velocity.

Navigation uncertainty results in an estimated error of ±3 cm/s for the acoustic reference velocity between each station

[1]Now at Atmospheric and Environmental Research, Incorporated. Cambridge, Massachusetts.

Paper number 7C0886.
0148-0227/88/007C-0886$05.00

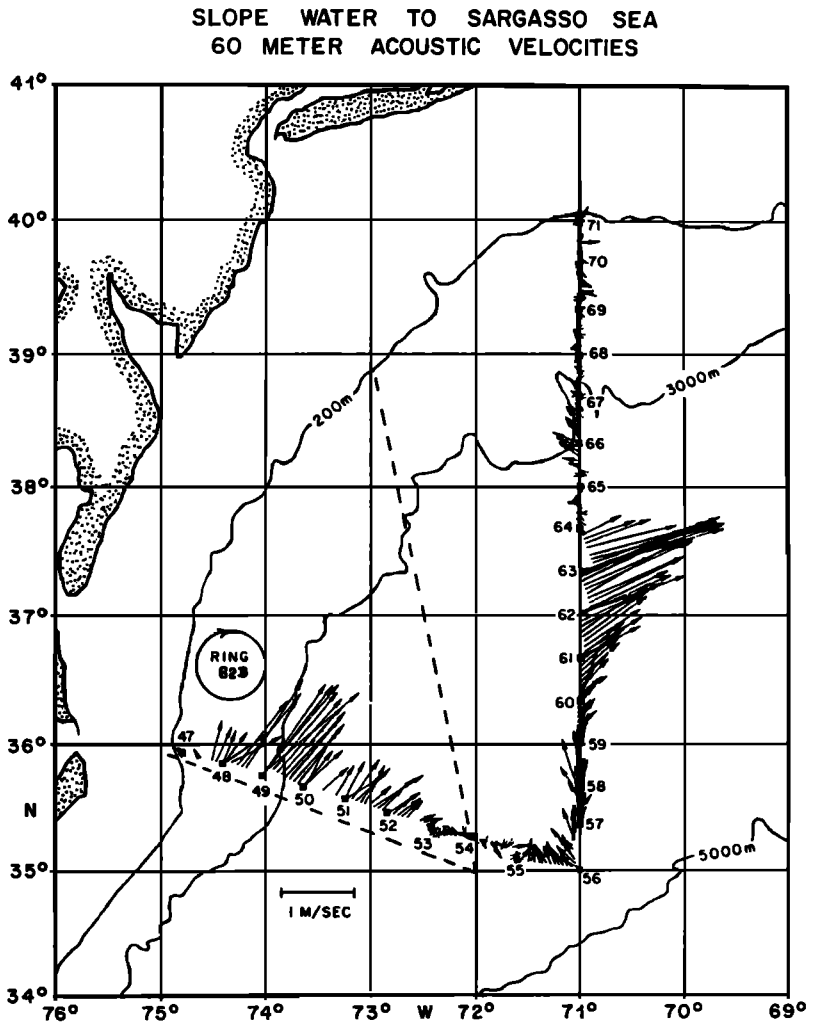

Fig. 1. CTD/O_2 station positions and some representative acoustic Doppler vectors from the 60-m depth bin, edited for clarity. The approximate location of warm-core ring 82B is also indicated. The dashed lines denote the sections discussed by JWP.

pair. In addition to this predicted noise level, there may be a systematic offset error of as much as 2.6 cm/s due to a slight misalignment of the transducers with the axis of the ship. This offset will produce an artificial velocity systematically to the right or left of the ship track. A complete discussion of these sources of error and the data reduction techniques appears in the work of *Pierce* [1986].

Throughout the discussion the section consisting of stations 47–56 will be known as the "south" section and stations 56–71 will be referred to as the "north" section (Figure 1). Plots of potential temperature, salinity, oxygen, and σ_θ appear in Figures 2 (south) and 3 (north). The Gulf Stream region is clearly identified by the strongly sloping isolines of all of the properties. Surface temperatures greater than 26°C and the subsurface salinity maximum (greater than 36.6 parts per thousand, or ppt) are both typical of the Gulf Stream at this time of year. In the Slope Water region to the north (stations 68–71, Figure 3), the intrusion of shelf and slope water is identified by inversions of temperature, salinity, and oxygen in the upper 100 m [*Stalcup et al.*, 1985]. At the Sargasso Sea corner of the triangular area (station 56), the Eighteen Degree Water has a thickness of about 175 m, as defined by $\theta = 17.9 \pm 0.3$°C and $S = 36.5 \pm 0.1$ ppt. An intriguing aspect of the region is the presence of the Deep Western Boundary Current (DWBC) and the nature of its crossing underneath the Gulf Stream. The DWBC is revealed in both the south and north sections by the deep oxygen maximum (>6.2 mL/L).

3. TECHNIQUE

Our two sections form a convenient triangular region, bounded by the 200-m isobath at stations 47 and 71 (Figure 1). Noting that *Beardsley and Boicourt* [1981] estimate the transport over the shelf to be 0.2 Sv, any transport across the shelf break should be insignificant relative to the huge fluxes across the south and north sections. Given the near-synopticity of the two sections, we assume conservation of mass within the area; the net mass flux across the two sections should be nearly in balance.

Using the 100-dbar reference velocity from the Doppler instrument, we apply geostrophy and calculate transports across the south and north sections. Not surprisingly, the two transports are out of balance: the south section has a net flux which is 50×10^9 kg/s larger than the north's. As was mentioned previously, we suspect that the acoustic velocities contain a small systematic offset to one side of the ship. Since the ship traverses the two sections in opposite directions, this

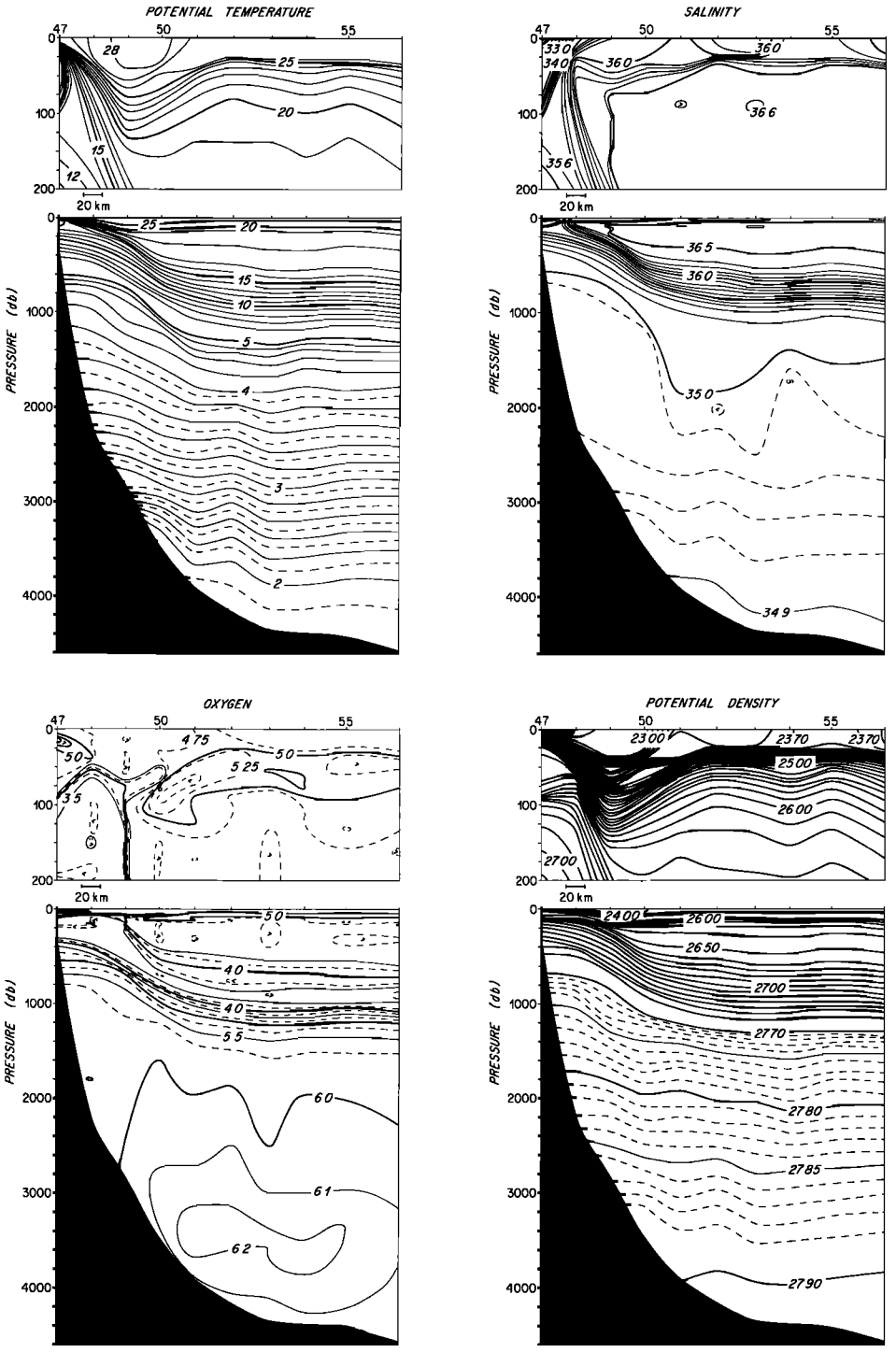

Fig. 2. Property distributions for the south section (approximately 73°W): (top left) potential temperature, (top right) salinity, (bottom left) oxygen, and (bottom right) σ_θ. Vertical exaggeration is 50–1.

error would consistently increase velocities along one section and decrease them along the other. By applying a correction of only 1.5 cm/s across both sections, the net transports are balanced: 170×10^9 kg/s across each. This level of systematic error is within the bounds to be expected. In the EN86 data set, we found this offset error to be 1.9 cm/s [JWP].

A random error component of ± 3 cm/s is still associated with our velocities, however. This level of noise implies an uncertainty of $\pm 13 \times 10^9$ kg/s and $\pm 15 \times 10^9$ kg/s in transport across the south and north sections, respectively. While these error bars are no doubt comparable with many historical transport estimates, we seek a technique to reduce them. By inspection of the property sections (Figures 2 and 3), isopycnals are chosen to divide the water column into 13 density layers. Following JWP, we attempt to resolve the major water mass features with these layers. Table 1 lists the chosen isopycnals, average depths, and transports across each section for each layer under "direct acoustic."

Assuming a small degree of cross-isopycnal flow, the transport within each layer should be in approximate balance be-

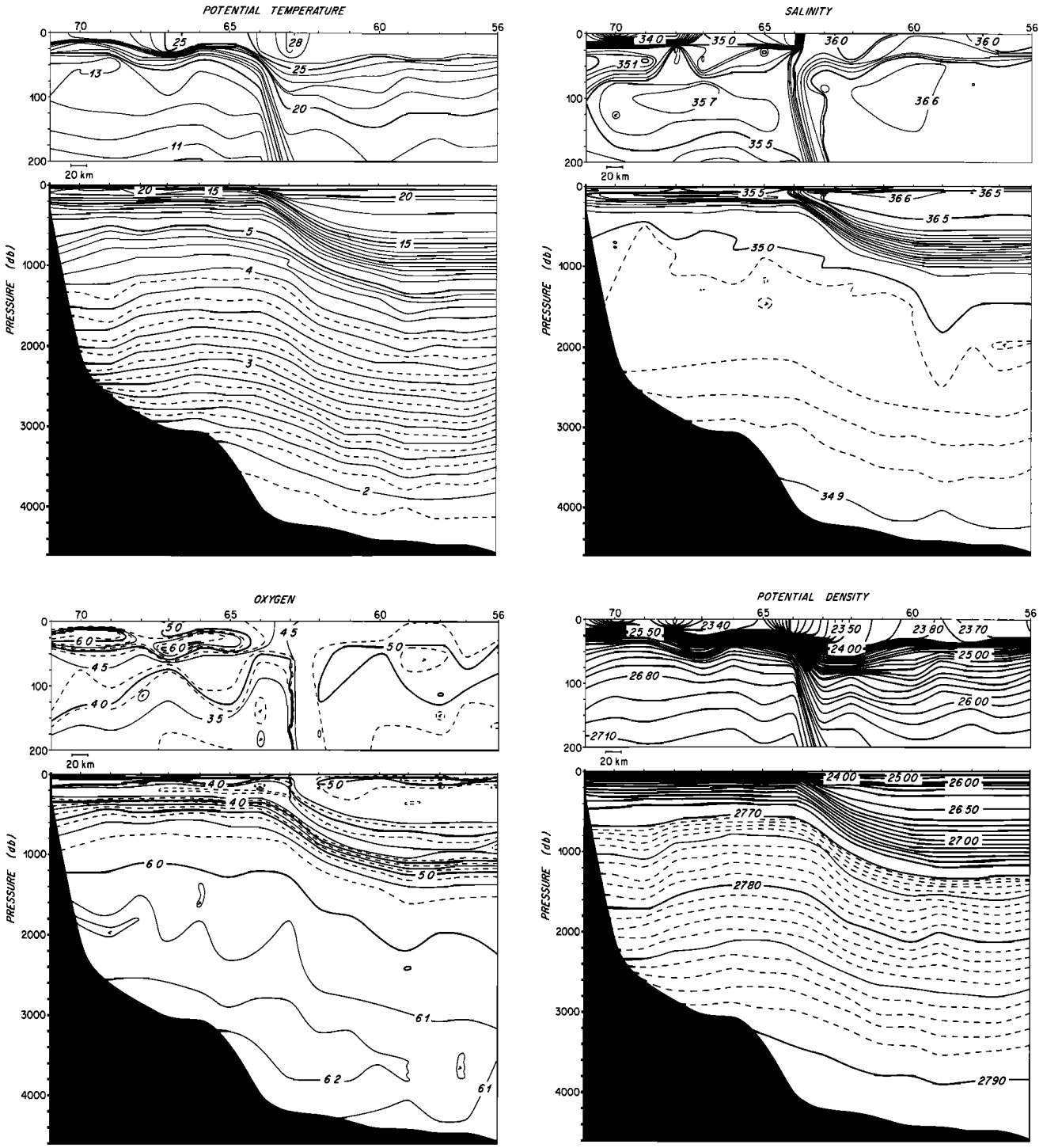

Fig. 3. Property distributions for the north section (on 71°W): (top left) potential temperature, (top right) salinity, (bottom left) oxygen, and (bottom right) σ_θ.

tween the south and north. Inspection of Table 1 indicates that the imbalances are in fact too large to be physically acceptable. To resolve this problem and improve our velocity estimates, we can get more information out of this data set through inverse techniques.

The inverse method follows the same form as procedures thoroughly developed by *Wunsch* [1978]. *Wunsch and Grant* [1982], and *Wunsch et al.* [1983]. The two classical principles of geostrophy and property conservation are applied in a formal and consistent manner while remaining within the error bars of the acoustic Doppler velocity estimates. Details of the method are omitted, since they are thoroughly described by *Pierce* [1986] as well as by JWP.

To within estimated errors, we require mass balance within each of our 13 layers. In addition, we require salt transport balance for each layer and oxygen conservation for all but the top two surface layers. Simultaneously with the application of these conservation constraints, our reference velocities must remain within the error bars of the acoustic Doppler velocities.

The complete system consists of a total of 63 constraint equations in 36 unknowns (24 horizontal reference velocities

TABLE 1. List of Isopycnals and Summary of Mass Transports Within Each Layer

Layer	σ_θ	Average Depth of Surface, km	Direct Acoustic		Combined Rank 33		Combined Rank 36	
			South	North	South	North	South	North
		surface						
1			5.2	4.8	5.2	4.7	5.1	4.7
	24.000	0.020						
2			4.4	5.7	4.3	5.6	4.2	5.6
	25.000	0.051						
3			31.1	28.8	29.2	28.9	29.5	28.4
	26.500	0.291						
4			31.4	29.0	29.9	28.8	29.9	28.4
	27.000	0.541						
5			13.2	12.7	12.6	12.0	12.4	12.1
	27.300	0.684						
6			6.8	8.2	6.6	7.7	6.3	7.7
	27.500	0.784						
7			8.9	10.1	8.4	8.3	8.0	9.1
	27.700	1.022						
8			9.1	11.6	8.7	8.9	7.9	9.9
	27.760	1.384						
9			10.8	14.8	9.5	11.5	8.9	12.3
	27.800	1.827						
10			16.0	16.7	13.7	12.8	13.1	13.3
	27.850	2.452						
11			11.5	8.6	9.1	6.2	9.3	6.2
	27.880	2.879						
12			3.8	7.1	4.9	6.1	5.0	5.1
	27.898	3.219						
13			17.5	11.5	11.1	11.7	12.6	9.6
		bottom						
Section totals			170.0	170.0	153.0	153.0	152.0	152.0

Units are 10^9 kg/s $\simeq 1.03 \times 10^6$ m^3/s, positive north and east.

plus 12 cross-isopycnal velocities). The degree of independence among the constraints is defined by the rank; if the rank is actually equal to 36, then the system is a fully determined one, a regression problem. If the rank is less than 36, we have a rank deficient or inverse problem. Typically, there is some uncertainty as to the rank of a problem; in our case, we find that the rank lies somewhere between 33 and 36, nearly a fully determined problem.

The singular value decomposition (SVD) method [*Wunsch*, 1978] is used to solve our system. One of the advantages of the SVD technique is the information it provides regarding the contribution of each constraint to the solution. Table 2 summarizes the amount of information that each type of constraint contributes to the solution. In the rank 33 and 36 solutions, we note that the mass and salt balance equations contribute roughly equal amounts; this is not surprising, since mass and salt transport are highly correlated. Oxygen contributes less information, since we only require near-conservation from it. The dominant contributions come from the acoustic Doppler constraints: they are still providing most of the information for our solution. Note how much less information is available without the acoustics: a pure hydrographic inversion is typically a largely underdetermined problem. The direct acoustic column, on the other hand, reminds us that the use of only the Doppler data is also an underdetermined problem. Each set of constraints contributes significantly to our result.

4. Results

The uncertainty between the rank 33 and 36 solutions is the largest formal uncertainty in the solution. The differences between the two are slight; the solution remains very stable between ranks 33 and 36. Table 1 summarizes the mass transport results and compares them to the direct acoustic case. The total transports for the combined inversions are decreased by about 20 Sv from the direct acoustic case, while the north versus south fluxes for each layer reveal greatly reduced imbalances. The imbalances that do exist are largely explained by cross-isopycnal mass transfers that are explicitly solved for by the inverse calculation.

Figure 4 presents the values of the rank 33 and 36 reference velocities relative to the direct acoustic values; these are the residuals left in the set of velocity constraints. In the rank 33 case the acoustic values are maintained with a bias error of -1.7 cm/s across the south section and 0.4 cm/s across the north, with a random component of ± 3 cm/s overall. For rank 36 the offsets are -2.3 cm/s and 0.7 cm/s, and the random error is -1.9 cm/s. These offsets are of the correct sign and magnitude to be explained by the transducer angle error, while the random components are consistent with our estimate of navigational uncertainty. The representative error bars shown in Figure 4 indicate our formal confidence in any particular reference velocity; this is typically 1–2 cm/s.

The reference velocity that deviates the most from the

TABLE 2. Contribution of Each Category of Constraint to the Total Solution

Constraints	Direct Acoustic	Rank 33	Rank 36
Mass layers 1–13 & total	···	5.05	5.39
Salt layers 1–13 & total	···	4.93	5.10
Oxygen layers 3–13	···	2.94	3.39
Total property conservation	···	12.92	13.88
Acoustic velocities	24	20.08	22.12
Total rank	24	33	36

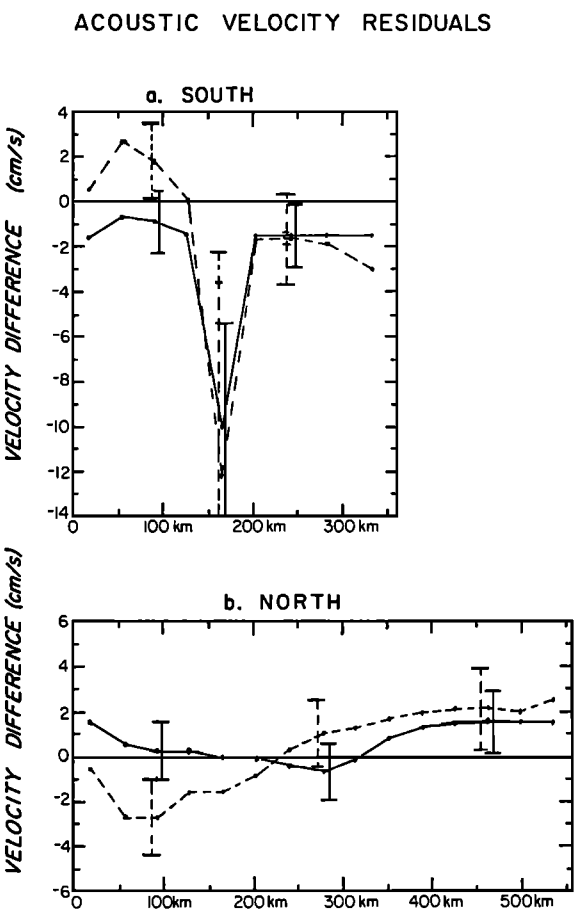

Fig. 4. Differences between the rank 36 (solid) and rank 33 (dashed) solutions from the direct acoustic values. Two sets of error bars are shown for the rank 33 case; inner set is due to failure to resolve, while outer set includes additional error due to noise in the data. Error bars for the rank 36 solution are wholly due to noise, since this is the fully resolved case. (*a*) South section. (*b*) North section.

acoustic value is between stations 51 and 52 (fifth from left in Figure 4*a*). Inspection of the raw Doppler data reveals that between stations 51 and 52 the data return was at its lowest; at the 60-m depth bin, only 46% of the emitted pulses were being received. The amount of scattering material present was at a minimum, and apparently the accuracy of the Doppler estimate begins to be affected at this level. The difficulty that the combined inverse technique had in resolving this particular velocity has taught us something about the quality of the acoustic Doppler data.

Useful information regarding the structure of our solution can also be gained by study of the residuals left in the property constraint equations (Figure 5). These mass, salt, and oxygen residuals represent those aspects of the data set which have not been explained by the solution; if we feel that we have extracted all the useful information out of our data, the residuals should appear to be random noise. The mass residuals do not quite appear random; some sort of structure with depth is apparent. This might indicate some missing physics from the model, something beyond pure geostrophy. Considering we are at the level of $\pm 0.1 \times 10^9$ kg/s, however, it does not seem worthwhile to attempt a more sophisticated model. Note that the residuals for oxygen, however, do in fact correspond well with ideas regarding the nonconservation of oxygen: production of O_2 near the surface and consumption in the deeper water.

Given the slight differences between the rank 33 and 36 solutions, the velocity sections are nearly indistinguishable by eye. We present in Figure 6 the rank 33 solutions. Fig. 7 summarizes the mass transport accumulated across the south and north sections for both the rank 33 and 36 solutions.

5. Discussion

Through the inverse procedure we have achieved our best estimate of the synoptic flow field off of Cape Hatteras in August 1982. As with most other estimates, this description of the Gulf Stream does not represent an average condition; the region is well known for its variability. The velocity sections (Figure 6) reveal a Gulf Stream core moving at speeds as high as 120 cm/s across the south and 130 cm/s across the north section. The Gulf Stream flow extends to the bottom on both sections, and to the north we see an especially strong eastward flow at the bottom. In the deep water of the south section, two components of southwestward flow of high oxygen water are evident, identifying the Deep Western Boundary Current (DWBC). The stronger of these is just east of the deep Gulf Stream, between stations 52 and 53, while another component is west of the stream. To the north, the deep westward flow appears in several places but is concentrated between stations 64 and 69. The sense of the vertical shear is such that shoreward of the 3000-m isobath the westward flow increases upward from the bottom, while the opposite holds seaward of 3000 m. Throughout the Slope Water region the deep shear is weak, and the flow is generally barotropic and to the southwest. These characteristics of the Slope Water circulation are consistent with the long-term mean flow across 70°W presented by *Hogg* [1983], which also exhibits a region of surface-intensified southwestward flow, as one sees between stations 66 and 67. Along the north section the DWBC is primarily found to the north of the axis of the stream, while to the south the southwestward flow is found on either side of the stream. This splitting of the DWBC agrees with the observations of *Richardson and Knauss* [1971], who suggest that the deep Gulf Stream flow at the bottom is related to the separation of the DWBC into two components.

The total mass transport across both of our sections is 152 $\pm$ 1 $\times$ 10^9 kg/s (Table 1). The narrow range of uncertainty between the rank 33 and 36 solutions is another indication that the mass conservation assumption within our region is an excellent one. Figure 7 gives the total accumulated transport across both sections. To discuss Gulf Stream transport figures, we must first decide on a definition of the Gulf Stream. This is not a simple issue, and *Knauss* [1969] suggests that this is the largest source of discrepency among historical transport estimates. A convenient way of defining the edge is to look at where the transport per unit width changes direction. This tends to work well with the northern edge, but to the south the total transport may not change its sign. To define the Sargasso Sea edge, we look for a change in direction of the surface velocities rather than a change in the total top-to-bottom transport.

We settle upon a definition which is the total net transport between stations 48 and 54 along the south section and that between stations 60 and 65 to the north. This means that the width of the stream is roughly equal at both locations and consistent with previous definitions of the stream. To compare our mass transport figures with historical volume transports,

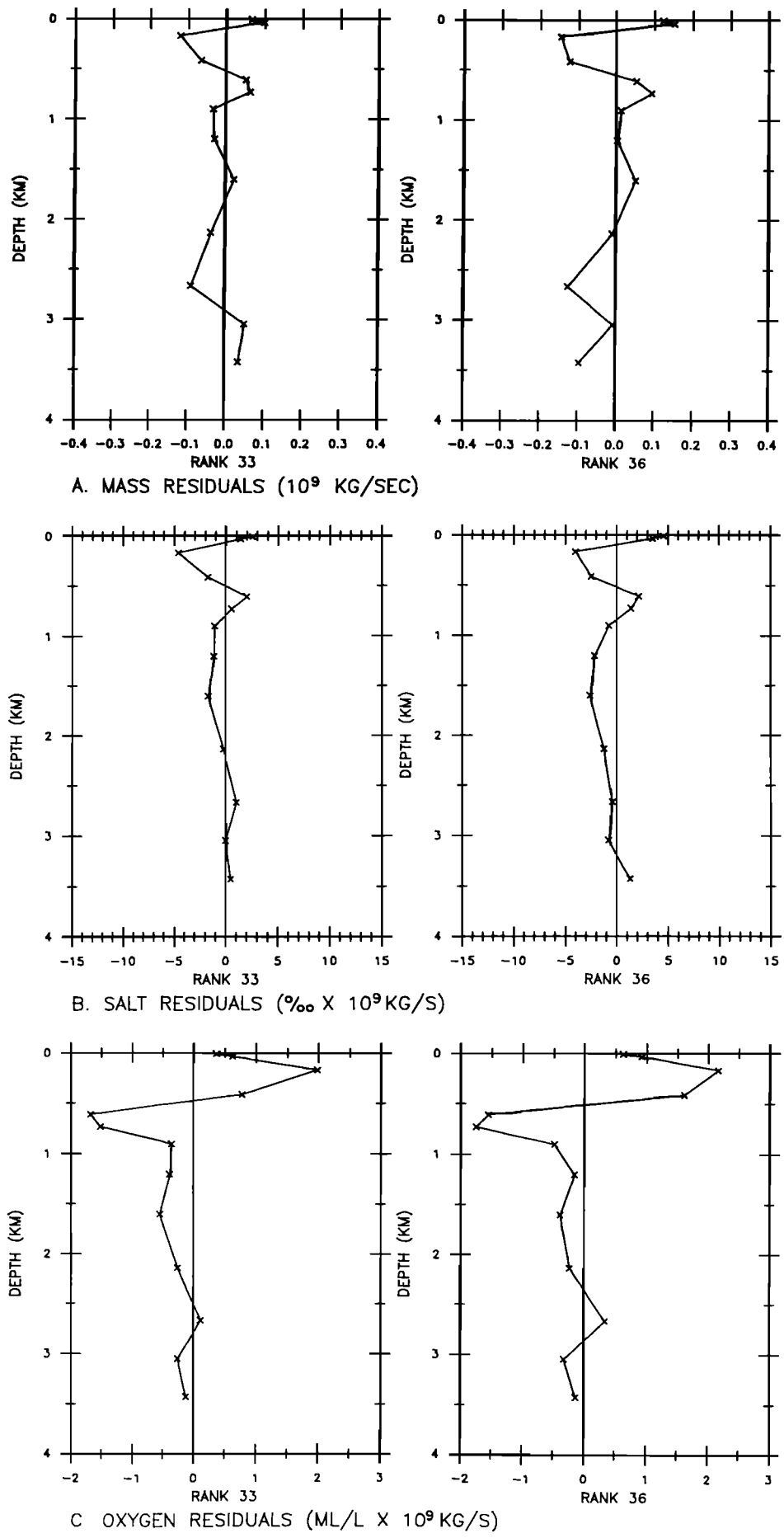

Fig. 5. Residuals left in the conservation constraints for (*a*) mass, (*b*) salt, and (*c*) oxygen transport. Properties are scaled using equivalent units.

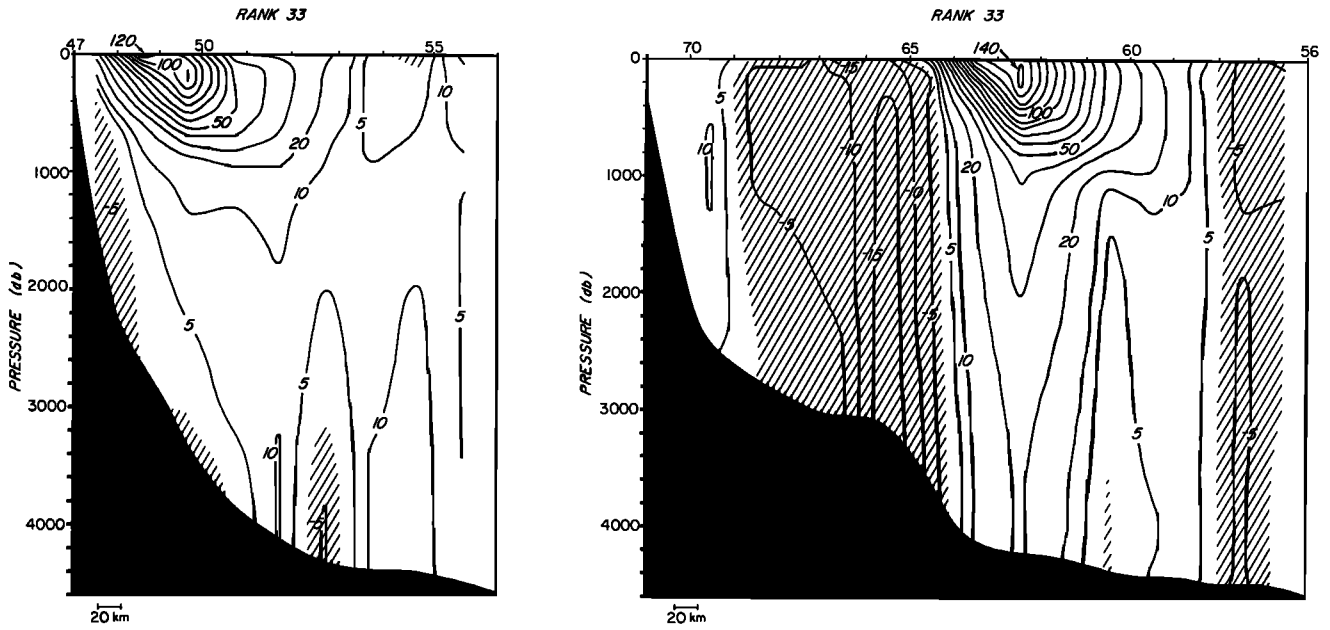

Fig. 6. Velocity results (in centimeters per second) normal to the (*a*) south and (*b*) north sections.

we use the approximation that 10^9 kg/s $\simeq$ 1.03 Sv. The result is a Gulf Stream transport of 113 $\pm$ 2 Sv across the south section and 156 $\pm$ 4 Sv across the north. This downstream increase in transport translates to an average downstream rate of increase of 13.5 $\pm$ 0.6 Sv/100 km. This increase is due to approximately equal additions of Slope Water from the north and the recirculation south of the stream. Note that 33 Sv out of the total increase of 43 Sv is depth independent; the increase in transport is predominantly barotropic. The surface manifestation of this recirculation can be seen directly in Figure 1 with addition of Sargasso Sea Water into the southern corner of the pie-shaped region and Slope Water inflow to the north of station 64.

We present Figure 8 and Table 3 to compare our transport figures with some historical estimates. From Cape Hatteras at 75°W to the Grand Banks at 65°W, the Gulf Stream transport increases dramatically. In Figure 8, both the present EN88 estimates and the EN86 estimates from JWP are plotted as solid circles. These are the only points with error bars shown, since the inverse technique provides them explicitly, but certainly most of the historical estimates deserve larger error bars than these. Compared with most of the estimates located closest to our sections, our transports are larger. This is particularly true of our estimates at 72.5°W and 71°W; these imply a greater downstream increase in transport than historical notions. Using some of the points plotted in Figure 8, *Knauss* [1969], for example, predicts a downstream rate of increase of 7%/100 km; this translates to 10 Sv/100 km for our region, while we measure 14 Sv/100 km (lines marked KN and PJ, respectively, in Figure 8). Moreover, in both the EN86 and EN88 cases, we note a strong southwestward flow of Slope Water which contributes nearly half of the increase in transport, equal to the expected recirculation gyre on the Sargasso side.

Halkin and Rossby [1985] recently performed 16 crossings of the Stream at 73°W with the Pegasus vertical profiler over a 2.5-year period. Since their useful data only extended down to 2000 dbar, their results are not included in Table 3. The Pegasus results are valuable, however, in demonstrating the variability of the transport in the region; their 0/2000-dbar mean transport is 88 Sv but has a standard deviation of $\pm$17 Sv. Our results at 73.3°W are quite consistent with this: we find a 0/2000-dbar transport of 95 $\pm$ 2 Sv. Our values are larger than the mean yet well within the range of variability expected for the region. Another recent synoptic transport estimate which only went from 0/2000 dbar has been made by *Johns* [1984]; using the POGO transport float and hydrographic sections, she quotes 126 Sv at 70.5°W, consistent with our 0/2000-dbar figure of 117 $\pm$ 2 Sv at 71°W. *Halkin and Rossby* [1985] also measure downstream increase of transport and report 15 Sv/100 km (marked HR in Figure 8), in line with our estimate of 14 Sv/100 km (PJ in Figure 8). Since the HR line is again only for 0/2000 dbar, only the slope of this line is relevant, not its position relative to PJ. Both HR and

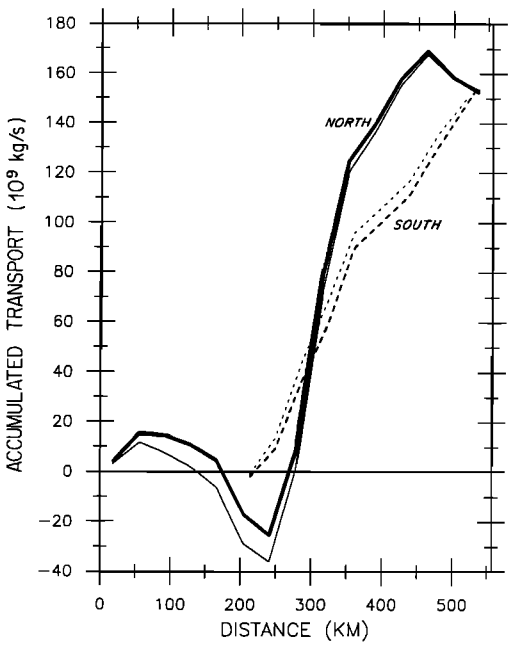

Fig. 7. Total accumulated transport across the south (dashed) and north (solid) sections. Heavier lines in either case indicate rank 36 solution; lighter lines are rank 33. Distance scale begins at the Slope Water end of each section.

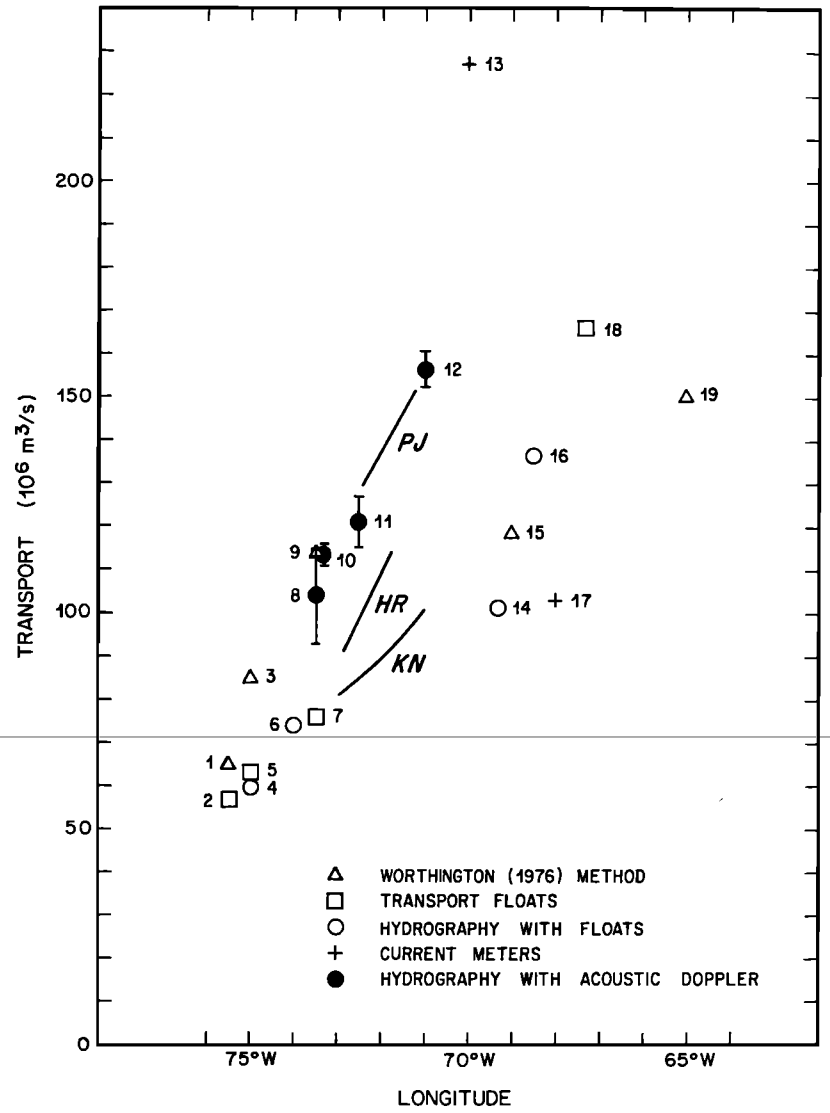

Fig. 8. Gulf Stream transport estimates versus longitude as listed in Table 3. Also shown are lines representing downstream increase in transport: the *Knauss* [1969] 7%/100 km estimate (KN), the *Halkin and Rossby* [1985] 15 Sv/100 km estimate (HR), and the present study's 14 Sv/100 km estimate (PJ).

the present study suggest that the Gulf Stream transport increases more quickly after Cape Hatteras than is suggested by historical notions.

We also calculate a transport for the DWBC by summing up the components of deep, high-oxygen water moving southwest within the density layers 11 and 12 (Table 1). The result is 3 Sv across the south leg and 5 Sv for the north; we express our estimate as 4 ± 1 Sv. Historical estimates of the DWBC transport have varied tremendously, probably owing to both time variability and differing techniques. *Richardson* [1977] reviews a number of historical estimates and calculates a mean of 16 ± 14 Sv. Perhaps the most reliable estimate of the mean is that of *Hogg* [1983], who used long-term current meters at 70°W and reported 10 Sv of classic DWBC transport. Our value is below most estimates but still consistent with the apparent variability of the feature. JWP found a DWBC transport of $9 \pm$ Sv, closer to the *Hogg* [1983] estimate.

6. Final Remarks

We have achieved a complete description of the synoptic velocity field in the region through the combined inversion of the acoustic Doppler and CTD/O_2 data. The errors in the acoustic Doppler velocities are dominated by the ship's navigational uncertainties; improvements in navigation could greatly improve the quality of the acoustic data. More accurate LORAN or a completely operational global positioning system might reduce the random errors to the ± 1 cm/s level. Reduced random error will allow for a better calibration and a subsequent reduction of systematic error. The latter must be constrained now by mass budgets; failure to do so will result in large errors in transport which grow linearly with the length of the section.

Since we have a region enclosed by hydrographic sections and a continental boundary, we are able to write property conservation equations appropriate for the inverse procedures introduced by *Wunsch* [1978]. Our problem is nearly a fully determined one; in this sense it differs greatly from typical hydrographic inversions which tend to be grossly underdetermined. Rather than being the only source of information, the property constraints offer us additional information to refine our acoustic velocities.

Similar methods applied to an area with less time variability and smaller velocities could produce even greater accuracy. In this region the assumption that the Gulf Stream has not

TABLE 3. Variation of Gulf Stream Transport Downstream

Source	Longitude, °W	Method	Transport, 10^6 m^3/s
Worthington [1976]	75.5	W	65
Knauss [1969]	75.5	T	57
Worthington [1976]	75	W	85
Barrett [1965]	75	G	60
Richardson and Knauss [1971]	75	T	63
Worthington and Wright [*Knauss*, 1969]	74	G	74
Knauss [1969]	73.5	T	76
Joyce et al. [1986]	73.5	AD	104 ± 11*
Worthington [1976]	73	W	114
Present work	73.3	AD	113 ± 2*
Joyce et al. [1986]	72.5	AD	121 ± 6*
Present work	71	AD	156 ± 4*
Robinson et al. [1974]	70	CM	227
Warren and Volkmann [1968]	69.3	G	101
Worthington [1976]	69	W	118
Fuglister [1963]	68.5	G	137
Hall [1985]	68	CM	103
Barrett and Schmitz [1971]	67.3	T	166
Worthington [1976]	65	W	150

Transport estimation methods are as follows: W, *Worthington* [1976, p. 18] method; T, transport floats; G, hydrographic sections (deep floats or bottom reference); CM, current meters; AD, hydrographic sections (acoustic Doppler reference).

*Converted from 10^9 kg/s to 10^6 m^3/s assuming a density of 1030 kg/m^3.

varied substantially during the 4-day observation period is one limiting factor; *Halkin and Rossby* [1985], for example, have noted variations in transports of as much as 10 Sv over the course of 7 days. Second, we have neglected ageostrophic dynamics which could affect both the measured near-surface velocities as well as the thermal wind balance used to extend these measurements downward. The restrictions imply that further efforts to improve the accuracy of our estimate may not be warranted; we may have obtained as much useful information as possible out of this data set.

Acknowledgments. This work has been supported by National Science Foundation grant OCE 8501176. Thanks go to Barbara Grant for help with the inverse calculations, to the WHOI CTD group, Jane Dunworth, and Cleo Zani for collecting and processing data, and to Lorraine Barbour for drafting some of the figures. Woods Hole Oceanographic Institution contribution 6569.

REFERENCES

Barrett, J. R., Jr., Subsurface currents off Cape Hatteras, *Deep Sea Res.*, *12*, 173–184, 1965.

Barrett, J. R., Jr., and W. J. Schmitz, Jr., Transport float measurements and hydrographic station data from three sections across the Gulf Stream near 67°W, *Tech. Rep. WHOI-71-66*, Woods Hole Oceanogr. Inst., Woods Hole, Mass., 1971.

Beardsley, R. C., and W. C. Boicourt, On estuarine and continental-shelf circulation in the Middle Atlantic Bight, in *Evolution of Physical Oceanography, Scientific Surveys in Honor of Henry Stommel*, edited by B. A. Warren and C. Wunsch, MIT Press, Cambridge, Mass., 1981.

Fuglister, F. C., Gulf Stream '60, *Prog. Oceanogr.*, *1*, 265–383, 1963.

Halkin, D., and T. Rossby, The structure and transport of the Gulf Stream at 73°W, *J. Phys. Oceanogr.*, *15*, 1439–1452, 1985.

Hall, M. M., Horizontal and vertical structure of velocity, potential vorticity and energy in the Gulf Stream, *Tech. Rep. WHOI-85-16*, 165 pp., Woods Hole Oceanogr. Inst., Woods Hole, Mass., 1985.

Hogg, N. G., A note on the deep circulation of the western North Atlantic: Its nature and causes, *Deep Sea Res.*, *30*, 945–961, 1983.

Johns, E., Geostrophy and potential vorticity in the Gulf Stream northeast of Cape Hatteras, N. C., Ph.D. thesis, 222 pp., Univ. of R. I., Kingston, 1984.

Joyce, T. M., D. S. Bitterman, Jr., and K. Prada, Shipboard acoustic profiling of upper ocean currents, *Deep Sea Res.*, *29*, 903–913, 1982.

Joyce, T. M., C. Wunsch, and S. D. Pierce, Synoptic Gulf Stream velocity profiles through simultaneous inversion of hydrographic and acoustic Doppler data, *J. Geophys. Res.*, *91*, 7573–7585, 1986.

Knauss, J. A., A note on the transport of the Gulf Stream, *Deep Sea Res.*, *16*, suppl., 117–123, 1969.

Olson, D. B., R. W. Schmitt, M. A. Kennelly, and T. M. Joyce, A two-layer diagnostic model of the long-term physical evolution of warm-core ring 82B, *J. Geophys. Res.*, *90*, 8813–8822, 1985.

Pierce, S. D., Gulf Stream velocity structure through combined inversion of hydrographic and acoustic Doppler data, *Tech. Rep. WHOI-86-41*, 64 pp., Woods Hole Oceanogr. Inst., Woods Hole, Mass., 1986.

Richardson, P. L., On the crossover between the Gulf Stream and the western boundary undercurrent, *Deep Sea Res.*, *24*, 139–159, 1977.

Richardson, P. L., and J. A. Knauss, Gulf Stream and western boundary undercurrent observations at Cape Hatteras, *Deep Sea Res.*, *18*, 1089–1109, 1971.

Robinson, A. R., J. R. Luyten, and F. C. Fuglister, Transient Gulf Stream meandering, I, An observational experiment, *J. Phys. Oceanogr.*, *4*, 237–255, 1974.

Stalcup, M. C., T. M. Joyce, R. L. Barbour, and J. A. Dunworth, Hydrographic data from warm core ring 82B, *Tech. Rep. WHOI-85-29*, 225 pp., Woods Hole Oceanogr. Inst., Woods Hole, Mass., 1985.

Warren, B. A., and G. H. Volkmann, Measurement of volume transport of the Gulf Stream south of New England, *J. Mar. Res.*, *26*, 110–126, 1968.

Worthington, L. V., On the North Atlantic Circulation, *John Hopkins Univ. Oceanogr. Stud.*, *6*, 110 pp., 1976.

Wunsch, C., The general circulation of the North Atlantic west of 50°W determined from inverse methods, *Rev. Geophys.*, *16*, 583–620, 1978.

Wunsch, C., and B. Grant, Towards the general circulation of the North Atlantic Ocean, *Prog. Oceanogr.*, *11*, 1–59, 1982.

Wunsch, C., D. Hu, and B. Grant, Mass, heat, salt, and nutrient fluxes in the South Pacific Ocean, *J. Phys. Oceanogr.*, *13*, 725–753, 1983.

T. M. Joyce, Woods Hole Oceanographic Institution, Woods Hole, MA, 02543.

S. D. Pierce, Atmospheric and Environmental Research, Inc., 840 Memorial Drive, Cambridge, MA 02139.

(Received August 19, 1987;
accepted October 20, 1987.)